

RESEARCH

Open Access



Enhanced soil aggregate stability limits colloidal phosphorus loss potentials in agricultural systems

Fayong Li^{1,2}, Xinqiang Liang^{1*} , Hua Li³, Yingbin Jin¹, Junwei Jin¹, Miaomiao He⁴, Erwin Klumpp⁵ and Roland Bol^{5,6}

Abstract

Background: Colloid-facilitated phosphorus (P) transport is recognized as an important pathway for the loss of soil P in agricultural systems; however, information regarding soil aggregate-associated colloidal P (P_{coll}) is lacking. To elucidate the effects of aggregate size on the potential loss of P_{coll} in agricultural systems, soils (0–20 cm depth) from six land-use types were sampled in the Zhejiang Province in the Yangtze River Delta region, China. The aggregate size fractions (2–8 mm, 0.26–2 mm, 0.053–0.26 mm and < 0.053 mm) were separated using the wet sieving method. Colloidal P and other soil parameters in aggregates were analyzed.

Results: Our study demonstrated that 0.26–2 mm small macroaggregates had the highest total P (TP) content. In acidic soils, the highest P_{coll} content was observed in the 0.26- to 2-mm-sized aggregates, while the lowest was reported in the < 0.053 mm (silt + clay)-sized particles, the opposite of that revealed in alkaline and neutral soils. Paddy soils contained less P_{coll} than other land-use types. The proportion of P_{coll} in total dissolved P (TDP) was dominated by < 0.053 mm (silt + clay)-sized particles. Aggregate size strongly influenced the loss potential of P_{coll} in paddy soils, where P_{coll} contributed up to 83% TDP in the silt + clay-sized particles. The P_{coll} content was positively correlated with TP, Al, Fe, and the mean weight diameter. Aggregate-associated total carbon (TC), total nitrogen (TN), C/P, and C/N had significant negative effects on the contribution of P_{coll} to potential soil P loss. The P_{coll} content of the aggregates was controlled by the aggregate-associated TP and Al content, as well as the soil pH value. The potential loss of P_{coll} from aggregates was controlled by its organic matter content.

Conclusion: We concluded that management practices that increase soil aggregate stability or its organic carbon content will limit P_{coll} loss in agricultural systems.

Keywords: Soil aggregate, Colloidal phosphorus, pH, Geometric mean diameter, Loss of phosphorus

Background

The loss of phosphorus (P) from agricultural soils has been identified as one of the main causes of eutrophication of lakes in the lower reaches of the Yangtze River in southern China [1]. Statistics have shown that major lakes and reservoirs in this area were eutrophic and

mesotrophic [2–4], and the Yangtze River Delta region accounted for 17% of the 10 Tg annual increase in soil P around the world [2]. In soil, colloidal P (P_{coll}) is the P fraction bound to colloids [5]. Colloidal particles are highly mobile and are effective adsorbents of organic and inorganic contaminants and nutrient elements, such as P, owing to the high specific surface area and charge density [6, 7]. Colloid-facilitated P transport is an important pathway for the migration of P into water bodies [5, 8, 9]. One study has reported that more than 75% of P in cultivated soil solution is combined with fine particles smaller

*Correspondence: liang410@zju.edu.cn

¹ College of Environmental and Resources Sciences, Zhejiang University, Hangzhou 310058, China

Full list of author information is available at the end of the article

than 240 nm [10]; similarly, 40–58% of molybdate-reactive P, with a size less than 450 nm in the water extract of grassland soil, demonstrates fine-grained P with a size of 25–450 nm [9]. Other studies have suggested that P_{coll} reached up to 50% of total P (TP) in surface runoff, rivers, and lakes [11], which may lead to environmental risks.

Soil aggregate stability plays a key role in controlling the erosion processes and the loss of soil nutrients [12–14]. Water-dispersible colloids in the soil adhere to soil aggregates, forming a stable system [15]. Colloids either can bind to soil aggregates, or be physically strained from water flowing through pores between aggregates [16, 17]. Some scholars determined the colloid content in 1–2 mm aggregates in 39 soils and revealed a significant positive correlation between the water-dispersible colloid content and clay content in soil aggregates [18]. Furthermore, they reported that water-dispersible colloid content was a function of total organic C and total clay. Other scholars modeled the release characteristics of colloids from soil aggregates, the attachment and detachment processes at the air–water interface, and flocculation and straining from interstitial water [19]. The release of colloids from aggregates may result in the disintegration of aggregates [20]. However, soil aggregation mainly depends on the availability of active mineral surfaces and the dispersion/flocculation behaviors of the colloidal components [21]. Meanwhile, the degree of clay colloid dispersion can be reduced by increasing the aggregate stability [18, 22, 23]. Therefore, the stability of soil aggregates directly affects the migration of soil colloids.

The retention of P in soil aggregates depends on the aggregate sizes and chemical properties [24, 25]. Notably, P has a relatively closed cycle, with most of the mineralized and dissolved P from microaggregates adsorbed onto unaggregated clay-sized particles (< 53 μm) or utilized by plants [26]. Reportedly, some studies have shown that the soil aggregate stability and size affect the soil P distribution [27–29]. Higher percentages of both water-extractable and Mehlich III-extractable P were observed in both the 0.50–0.25 and 0.25–0.125 mm aggregate fractions [30]. In contrast, reports have suggested that TP is the highest in small soil aggregates [31], or the TP content is uniform in soil aggregates of all sizes, whereas available P is higher in small soil aggregates [32]. Soil aggregation could reduce the loss of organic P in aggregates and increase the adsorption of inorganic P by silt and clay particles [26]. Meanwhile, the P forms in soil aggregates may vary with different particle sizes and land-use types [24, 33]. For example, a study has indicated that aluminum oxide bond P (Al–P) is mainly dominated by soil aggregates < 1 mm; those of 2–8 mm were mainly iron oxide bond P (Fe–P) and calcium oxide bond P (Ca–P) [34]. Other investigators have claimed

that the labile P in macroaggregates was higher under native land-use than other land uses, further confirming that soils under native use contained more Ca-bound P in macroaggregates than the disturbed soils [35]. These studies provide the first basis for the better understanding the relationship between soil aggregates and P.

To date, information on the P_{coll} content and its loss potential from aggregates remains limited. The impact of the aggregation process on the P_{coll} content in soils remains unclear. Moreover, the composition and structure of soil aggregates vary under different land-use management [36, 37]. There are fewer large-sized aggregates present in rice soil than dryland due to long-term flooding and anaerobic conditions that cause the macroaggregates to be dispersed [36, 38]. In addition, alternation between dry and wet conditions generally destroys macroaggregates and enhances the decomposition of organic carbon in paddy soils [39]. Therefore, we suspected that the content of P_{coll} in the macroaggregates of paddy soils was less than dryland soils, mainly existing in microaggregates and small particles, with a higher loss potential.

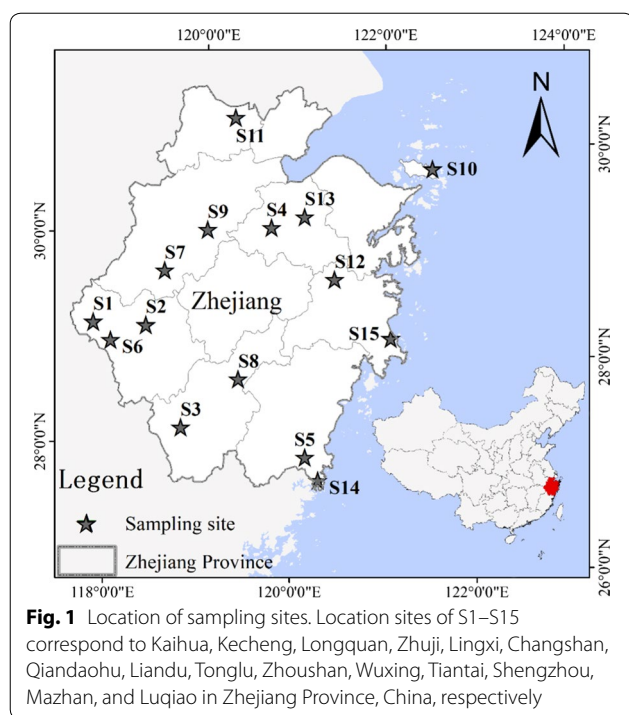
This study mainly aimed to understand the effect of soil aggregate stability on soil P_{coll} content and its loss potential, and to assess the core environmental factors affecting P_{coll} in soil aggregates. Hence, we collected soil samples from 15 sites and 6 land-use types in the Yangtze River Delta region, Zhejiang Province for aggregates and P_{coll} analysis. Firstly, we isolated the different-sized aggregates in the soil samples. Secondly, we determined the P_{coll} , total carbon (TC), TP, total nitrogen (TN), Al, Fe, and Ca content in each aggregate size fractions. We hypothesized that (1) larger sized aggregates have higher TP and P_{coll} content; (2) aggregates with a higher TC content have lower loss potential of P_{coll} , and (3) land-use management with single rice has a higher loss potential of P_{coll} .

Materials and methods

Soil sampling and preparation

In total, soils with different land-use types (Fig. 1) were collected from 15 sites, which were almost evenly distributed in the Zhejiang Province (an area of 1,055,000 km^2). Information on specific sampling points is presented in Table 1. The 15 sampling points covered six land-use types including orchards, single cropping rice, double-cropping rice, rice–rape rotation, rice–wheat rotation, and vegetables, generally established in the past 5 years.

Soil samples of 0–20 cm were collected from typical fields (long-term farmland with conventional fertilization by local farmers) in May 2018 during the second season of rotation systems and in other land-use types. Two samples, with three replicates, were obtained at intervals of 1000 m at each site with the same land-use type.



Next, the replicates were brought back to the laboratory and mixed. Then, the mixed soil samples from each site were divided into four equal parts by the diagonal quartering method and maintained for a follow-up test. All samples were air-dried and separated into two parts: one was finely milled and sieved through a 2-mm mesh to determine basic physical and chemical properties, and the other was carefully broken into small pieces manually and passed through an 8-mm sieve for aggregate separation and P_{coll} determination.

Aggregate separation and determination

Aggregate size distribution was determined for each soil sample using a modified wet sieving method [40]. Briefly, 50 g of unground soil, passed through an 8-mm sieve, was carefully placed above a nest of three sieves (2 mm, 0.26 mm, and 0.053 mm). Then, the sieves were submerged for 20 min in 2.5 L deionized water at room temperature and oscillated 300 times for 10 min with a 30-mm amplitude to separate aggregate fractions. Thus, four aggregate fractions were obtained on each sieve: large macroaggregates (2–8 mm), small macroaggregates (0.26–2 mm), microaggregates (0.053–0.26 mm), and (silt + clay)-sized particles (<0.053 mm) [41]. Aggregates of each size were carefully removed from the sieve and placed into a beaker. The water used for wet sieving was left to rest for 48 h, silt and clay particles were collected, and the supernatant was used to determine total dissolved P (TDP), truly soluble P (TSP), and P_{coll} content.

All aggregates were oven-dried at 65 °C for 48 h, weighed, and placed in a zip lock bag. To obtain water-stable aggregates, the sediment concentration was subtracted from that obtained by wet sieving as sand was not considered a component of water-dispersible aggregates [40]. The sand content was determined by the following process: 5 g of the dry aggregates obtained above were weighed, dispersed into 30 mL 5 g L⁻¹ hexametaphosphate solution, placed into an ultrasonic cleaner, and dispersed for 30 min. The suspension was then poured through a nest of sieves. The residue left on the 0.053-mm sieve represented the sand content of each sized aggregate. After collection, sand was dried at 65 °C and weighed.

Soil pH was determined with a glass electrode pH meter (PHS-3C, Shanghai) using a soil-to-water ratio of 1:5. Soil cation exchange capacity was measured with ammonium acetate (12.5 mL 1 M NH₄OAc, 2.5 g soil) [42]. Soil and aggregate-associated TP was determined by H₂SO₄–HClO₄ digestion and evaluated using the molybdenum-blue colorimetric method [43]. Soil particle size distribution was determined by the hydrometric method according to an international soil texture classification standard. Soil- and aggregate-associated TC and TN were determined using an elemental analyzer (dry combustion with Vario MAX CNS, Elementar, Germany). Soil- and aggregate-associated Al, Fe, and Ca were determined by inductively coupled plasma mass spectrometry (ICP-MS) after digestion with 5 mL HNO₃ (16 M), 1 mL HClO₄ (12.4 M), and 1 mL HF (23 M) for 12 h. All reagents were acquired from Sinopharm Chemical Reagent Co., Ltd.

Colloidal P was determined as described by Ilg [44]. Briefly, 10 g of unground soil was placed into a 250-mL flask, 80 mL deionized water was added. The sample was shaken at 160 rpm and 25 °C for 24 h. The supernatant was pre-centrifuged at 3000g for 10 min to remove coarse particles. After pre-centrifugation, the supernatant was filtered with a 1-μm microporous membrane, 5 mL of the primary filtrate was discarded, and the total filtrate was collected (sample I). This suspension included the colloidal and dissolved components. The filtrate was ultracentrifuged at 300,000g for 2 h to remove colloids (Optima TL, Beckman, USA; Sample II), and the residue at the bottom of the ultracentrifuge tube demonstrated the water-dispersible colloids. The TDP in Sample I and TSP in Sample II, in the solution, were determined after digestion with acidic potassium persulfate. The concentration of P_{coll} indicated the difference between TDP in Sample I and TSP in Sample II. Previous studies have shown that soil P through leaching and surface runoff was usually in the soluble form, that can pass through the 0.45–1 μm filter [45, 46]; therefore, in the present study, TDP including P_{coll} and TSP in aggregates was defined as the potential loss P, and the P_{coll} in TDP was defined as

Table 1 Basic chemical and physical properties of soil, and characterization of sites located in Zhejiang Province, China

Soils	S1	S2	S3	S4	S5	S6	S7	S8	S9	S10	S11	S12	S13	S14	S15
pH	3.9	4.5	5.1	5.2	5.3	5.5	5.9	6.2	6.4	6.6	7.0	7.1	7.3	7.4	7.8
TC (g kg ⁻¹)	8.4	3.3	13.1	11.1	14.8	4.5	10.8	10.3	7.7	17.5	13.5	5.2	20.2	9.0	14.1
TN (g kg ⁻¹)	1.5	0.5	1.5	1.4	1.7	0.6	1.4	1.3	0.9	2.0	1.4	0.7	2.2	0.9	1.7
TP (g kg ⁻¹)	1.3	0.2	0.5	0.8	1.1	0.3	0.8	0.7	1.6	0.6	0.5	0.3	1.1	0.9	1.0
CEC (cmol kg ⁻¹)	118.2	123.1	94.7	127.1	104.2	110.0	116.7	71.4	91.6	116.8	126.4	164.8	23.5	31.7	29.7
Sand (%)	12.4	45.5	71.8	56.9	16.4	70.6	18.9	69.4	78.5	32.4	21.4	70.7	46.0	16.6	9.8
Silt (%)	82.1	18.1	14.9	28.8	42.8	7.5	42.3	18.4	10.7	44.8	40.6	13.6	25.7	44.7	82.6
Clay (%)	5.5	36.4	13.3	14.3	40.9	21.9	38.8	12.2	10.8	22.8	38.0	15.8	28.3	38.7	7.7
Land use and vegetation	Orchard	Orchard	Single-cropping rice	Vegetable	Double-cropping rice	Orchard	Vegetable	Vegetable	Rice-rape rotation	Single-cropping rice	Single-cropping rice	Single-cropping rice	Single-cropping rice	Rice-wheat rotation	Rice-rape rotation
Mean annual temperature (°C)	16.4	17.0	16.5	16.3	18.0	17.7	17.0	17.8	16.5	16.0	15.8	16.8	16.4	14.0	16.9
Annual precipitation (mm)	1814.0	1657.0	895.6	1373.6	1670.1	1760.1	1489.0	1474.1	1552.0	1412.7	1200.0	1632.9	1446.8	1700.0	1486.0
Geographic coordinates (N, E)	118°16', 29°5'	118°50', 28°59'	119°4', 27°58'	120°23', 29°44'	120°22', 27°30'	118°26', 28°54'	119°8', 29°29'	119°46', 28°21'	122°41', 29°48'	122°17', 30°2'	120°11', 30°49'	122°0', 29°9'	120°47', 120°47'	120°28', 27°16'	121°30', 28°19'

TC total carbon, TN total nitrogen, TP total phosphorus, CEC cation exchange capacity

P_{coll} loss potential. TDP in the supernatant after 10 min wet sieving was considered as easy loss P.

Calculation of water-stable aggregate (WSA) size fractions

The proportion of WSA in each size fraction was obtained from Eqs. (1) and (2), as described by Alvaro-Fuentes [47]:

$$WSA_i = \frac{DSA_i - \text{Sand}_i}{\text{Total}_{\text{Soil}} - \sum_{i=1}^n \text{Sand}_i}, \quad (1)$$

$$(\text{silt} + \text{clay})\text{-sized fraction} = 1 - \sum_{i=1}^n WSA_i, \quad (2)$$

where i is the i th size fraction (2–8, 0.25–2, and 0.053–0.25 mm); dry soil aggregate (DSA_i) is the oven-dried mass of total, non-dispersed aggregates collected on each sieve; sand is the oven-dried mass of sand collected after dispersal in the hexametaphosphate solution on the 0.053 mm sieve; $\text{Total}_{\text{Soil}}$ is the oven-dried mass of soil (50 g) for aggregate separation.

Calculation of mean weight diameter (MWD) and geometric mean diameter (GMD)

The MWD and GMD of the aggregates were obtained by Eqs. (3) and (4) [48]:

$$\text{MWD} = \sum_{i=1}^n d_i \times WSA_i, \quad (3)$$

$$\text{GMD} = \text{EXP} \left[\frac{\sum_{i=1}^n WSA_i \log d_i}{\sum_{i=1}^n WSA_i} \right], \quad (4)$$

where i is the i th size fraction (2–8, 0.26–2, 0.053–0.26, and <0.053 mm) and d is the mean diameter of each size (0.053–2 mm). WSA_i include 2–8, 0.26–2, 0.053–0.25, and <0.053 mm WSA and (silt + clay)-sized fractions.

Contribution of aggregate-associated P_{coll} to TDP

The contribution rate (CR) was used to explore the impact of aggregate sizes on the P_{coll} loss potential, calculated using Eq. (5):

$$\text{CR}_i = \frac{\text{Agg_CP} \times WSA_i}{\sum_{i=1}^n \text{TDP}}, \quad (5)$$

where Agg_CP is the concentration of aggregate-associated P_{coll} (mg kg^{-1}), TDP is the concentration of total dissolved P (mg kg^{-1}), and i is the i th size fraction (2–8, 0.26–2, 0.053–0.26, and <0.053 mm).

Statistical analysis

Microsoft Excel 2016 and Origin 8.0 were used for data processing and cartography. Data were statistically analyzed using SPSS Statistics 22.0 (SPSS Inc. Chicago, USA) software. One-way ANOVA was performed using two samples from each site to examine differences of different variables as presented in Additional file 1: Tables S1, S2, and Figures S1, S2 and Table 3. Pearson correlation analysis was used to identify the relationship between aggregate-associated P_{coll} and other soil parameters. Stepwise linear regression was performed to evaluate the relationships between P indicators (content and loss potential of P_{coll}) and soil variables (pH, TP, TC, TN, C/N, Fe, Al, Ca, MWD, and GMD).

Results

Soil and aggregate characteristics

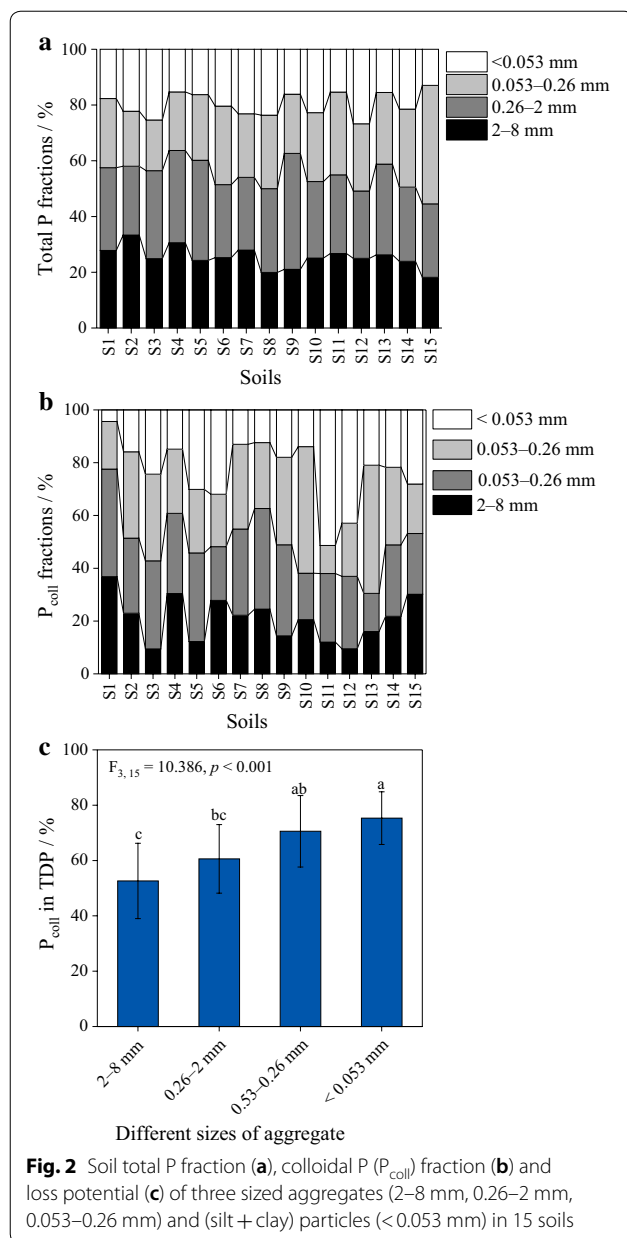
Within the 15 soils collected, ten were acidic soils, two were neutral soils, and three were alkaline soils (Table 1). There were six land-use types: orchard, single cropping rice, rice–rape rotation, vegetable, double-cropping rice, and rice–wheat rotation. The TC of the soils ranged from 3.32 to 20.19 g kg^{-1} ; TN ranged between 0.53 and 2.17 g kg^{-1} . TP varied from 0.23 to 1.64 g kg^{-1} . Soil pH values ranged between 3.95 and 7.83 (Table 1).

The DSA and WSA of larger macroaggregates (2–8 mm) generally increased with increasing pH values (Additional file 1: Figures S1 and S2, Table S2). Moreover, fractions of DSA and WSA (2–8 mm) in acidic soils ranged from 18.7 to 33.4% and from 10.5 to 47.1%, respectively. Conversely, fractions of DSA and WSA in alkaline soils ranged from 39.7 to 56.1% and from 38.1 to 55.6%, respectively. In contrast, size fractions of <0.053 mm particles gradually decreased with increasing soil pH values, while the average contents of <0.053 mm particles in acidic soils were 18.8 and 17.8%, compared with only 11.2% and 14.7% in alkaline soils, respectively.

The MWDs of acidic soils ($\text{pH} < 5.5$) were significantly smaller than those of alkaline soils ($P < 0.05$). The average MWD of acidic soils was 0.78 mm (Additional file 1: Figure S2), while that of neutral and alkaline soils was 1.36 mm. However, little difference in GMDs was observed between acidic (0.85 mm), and alkaline soils (0.91 mm).

Total and colloidal phosphorus content

Generally, the 0.26–2 mm aggregate fraction demonstrated the highest TP content, which accounted for 29.6% of the soil TP (Fig. 2a), and soil aggregates of 2–8 mm demonstrated the second-highest TP content. The TP content of (silt + clay)-sized particles was significantly lower than that of other fractions ($P < 0.05$,



Additional file 1: Table S1), which only accounted for 19.7% of the soil TP (Fig. 2a). Moreover, TDP, TSP, and P_{coll} contents were related to soil pH, and the highest TDP content was observed in 0.26–2 mm aggregates in most acidic soils and in (silt + clay)-sized particles in most alkaline soils ($P < 0.05$, Additional file 1: Table S1). In all soils, no significant difference was observed in the P_{coll} fractions between different aggregate sizes ($P > 0.05$; Fig. 2b). However, the aggregate content associated with P_{coll} was the highest in the 0.26–2 mm aggregates, and the lowest in the (silt + clay)-sized particles in acidic soils; in neutral and alkaline soils, (silt + clay)-sized particles

demonstrated the highest TDP and P_{coll} contents, followed by the 0.26–2 mm aggregates (Table 3).

Loss potential of colloidal phosphorus

After wet sieving, about 0.16–1.87% of the soil TP was lost in the supernatant as TDP, and P_{coll} accounted for 8.5–84.1% of the TDP (Table 2). The proportion of the easy loss P content in the various soils differed due to variations in soil physicochemical properties.

In general, the P_{coll} loss potential gradually decreased as the size of the soil aggregates increased (Fig. 2c). The P_{coll} loss potential was the lowest in 2–8 mm and 0.26–2 mm aggregates, with P_{coll} accounting for 52.6% and 60.6% of TDP, respectively. However, the P_{coll} loss potential of (silt + clay)-sized particles was the highest, with P_{coll} accounting for 75.3% of TDP (Fig. 2a). The CR value of (silt + clay)-sized particles was mostly larger than that of the other aggregate sizes, except for S7, S11 and S15; the CR of larger macroaggregates was lowest in most soils (Table 3).

Considering different land-use types, the P_{coll} content in the rice–dry land rotation and vegetable (VE) soils was significantly higher than that in paddy and orchard soils, regardless of different aggregate sizes (Fig. 3a). Higher P_{coll} content also was found in macroaggregates (>0.26 mm), except for the orchard soil (Fig. 3a). The colloidal P content in macro- and microaggregates in the paddy soils (including single cropping rice, and double-cropping rice) accounted for a relatively lower proportion of TDP ($P < 0.05$) than that in other land-use types (Fig. 3b). Overall, it accounted for only 39.3, 44.1, and 40.2% for the 2–8 mm, 0.26–2, and 0.053–0.26 mm aggregates in rice fields, respectively. Colloidal P in (silt + clay)-sized particles (<0.053 mm) in paddy soils accounted for a TDP proportion as high as 83.0%, significantly higher than that observed in the orchard and rice–dryland rotation systems (Fig. 3b). This indicated that the loss potential of P_{coll} was dominated by fine-grained and (silt + clay)-sized particles in paddy soils. However, the P_{coll} carried by all sized aggregates in dryland and rice–dryland rotation systems (orchard, rice–rape rotation, vegetable, and rice–wheat rotation) exceeded 50% of the TDP.

Factors affecting colloidal P content and loss potential

Correlation analysis revealed no significant correlations between P_{coll} and TC or TN (Table 4). The P_{coll} content was significantly and positively correlated with TP in all aggregate sizes except for (silt + clay)-sized particles (Fig. 4a). Soil pH positively correlated with the aggregate-associated P_{coll} content, but only significantly correlated with the P_{coll} content of (silt + clay)-sized particles ($P < 0.01$) (Fig. 4b). Additionally, Al and Fe significantly and positively correlated with P_{coll} in

Table 2 The total dissolved P (TDP), and truly soluble P (TSP), colloidal P, colloidal P/TDP, and ratio of TDP to soil total P (TP) in the supernatant of different soils after wet sieving

	TDP (mg kg ⁻¹)	TSP (mg kg ⁻¹)	Colloidal P (mg kg ⁻¹)	Colloidal P/TDP (%)	TDP/TP (%)
S1	5.71 ± 0.12	2.62 ± 0.34	3.1 ± 0.34	54.17	0.44
S2	3.49 ± 0.22	0.79 ± 0.18	2.7 ± 0.22	77.27	1.75
S3	6.35 ± 2.02	1.59 ± 0.45	4.76 ± 1.57	75.00	1.27
S4	3.41 ± 0.11	1.83 ± 0.11	1.59 ± 0.22	46.51	0.43
S5	6.03 ± 0.45	2.78 ± 0.34	3.25 ± 0.11	53.95	0.55
S6	2.14 ± 0.56	1.43 ± 0.67	0.71 ± 0.11	33.33	0.71
S7	1.27 ± 0.22	0.87 ± 0.11	0.4 ± 0.34	31.25	0.16
S8	5.48 ± 0.11	0.87 ± 0.11	4.6 ± 0.24	84.06	0.78
S9	29.92 ± 0.34	27.38 ± 0.11	2.54 ± 0.22	8.49	1.87
S10	3.73 ± 0.56	0.79 ± 0.15	2.94 ± 0.56	78.72	0.62
S11	5.4 ± 0.45	2.18 ± 0.62	3.21 ± 1.07	59.56	1.08
S12	1.90 ± 0.45	1.35 ± 0.56	0.56 ± 0.11	29.17	0.63
S13	7.06 ± 0.11	4.05 ± 0.11	3.02 ± 0.22	42.70	0.64
S14	6.59 ± 0.14	4.13 ± 0.90	2.46 ± 1.01	37.35	0.73
S15	6.43 ± 0.11	2.14 ± 1.01	4.29 ± 0.90	66.67	0.64

Data represent the average of three replicates ± standard deviations

total sizes of soil aggregate ($P < 0.05$) (Fig. 4c, d). However, only P_{coll} in 2–8 mm aggregate significantly and positively correlated with Al and Fe ($P < 0.05$). Moreover, P_{coll} was negatively correlated with C/P (Fig. 4e) and positively correlated with C/N (Fig. 4f). The forward results of the stepwise regression demonstrated that P_{coll} can be described by Al, TP, TN and MWD as follows: colloidal P = $-8.017 + 0.087\text{Al} + 10.598\text{TP} - 2.257\text{pH} - 5.977\text{MWD}$, ($R^2 = 0.605$, $P < 0.001$, Table 4).

The P_{coll} loss potential (P_{coll} in TDP) in total size of the soil aggregate negatively correlated with the TC, TN, pH, Ca, C/P, C/N ratios of aggregates (Table 4, $P < 0.05$). Considering different sizes, TC and TN significantly and negatively correlated with P_{coll} loss potential in 0.26- to 2-mm-sized aggregates. Except for (silt + clay)-sized particles, P_{coll} loss potential was significantly and positively correlated with Al ($P < 0.05$). P_{coll} loss potential in 2- to 8-mm-sized aggregates was significantly and positively correlated with Fe ($P < 0.05$). However, P_{coll} loss potential in 0.053- to 2-mm-sized aggregates negatively correlated with Ca ($P < 0.05$). The results of the stepwise regression demonstrated that the P_{coll} loss potential can be described by TC, Fe, MWD, and GMD as follows: colloidal P/TDP = $0.478 - 0.028\text{TC} + 0.015\text{Fe} + 0.413\text{MWD} - 0.363\text{GMD}$, ($R^2 = 0.539$, $P < 0.001$, Table 4).

Discussion

Total P in aggregates

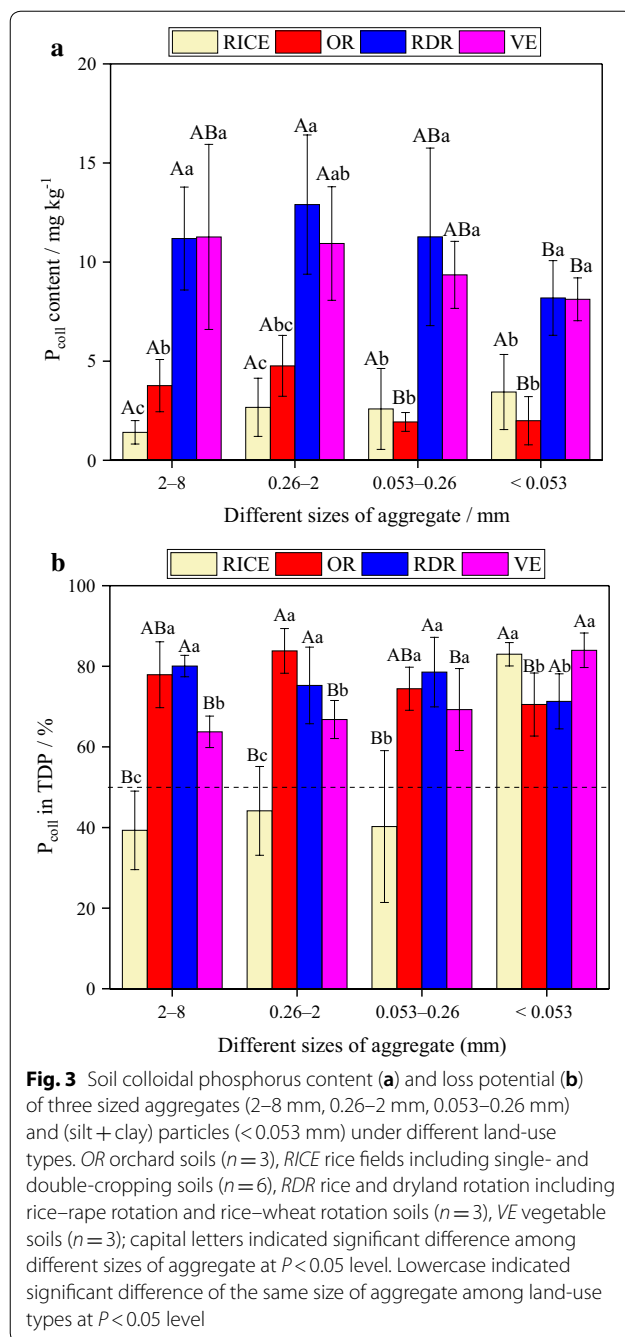
In our study, we observed that the TP content was the highest in macroaggregates of the 15 soils, while the TP content in the (silt + clay) particles was the lowest.

These results indicated that soil P was mainly carried by larger aggregates, which confirmed our hypothesis and were in line with those previously reported [28, 49, 50]. For examples, some scholars have observed that P tends to concentrate in large WSAs in long-term fertilization experiments in a reddish paddy soil [49], and others claim that aggregate-associated total organic C, TN, and TP are preferentially enriched in large WSAs (4.76–2.0 mm) [50], reporting that the TP proportion increased with increasing aggregate size for native lands [35]. Higher P levels may be associated with higher levels of TC and TN in large aggregates [50, 51]. Macroaggregates ($[(\text{Cl}-\text{P}-\text{OM})_x]_y$) are usually formed by organic matter, clay (Cl) and multivalent ions of P, and other substances [52, 53]. Organic matter (and associated P) is protected within stable aggregates against microbial degradation [54]. Moreover, it has been shown that the organic P forms that accumulate in soils are less available to enzymatic hydrolysis when bound to mineral surfaces [55, 56]. On the other hand, the aggregation promoted by organic matter counteracts the dispersion of the small mineral particles (mostly Fe and Al-(hydr) oxides where P is retained [57, 58]. Furthermore, this was validated by the positive correlation between aggregate-associated TP and TC, and the significant correlation between aggregate-associated TP and TN observed in this study (Additional file 1: Tables S2).

Table 3 The colloidal P content (mg kg⁻¹) of different-sized soil aggregates and the contribution rate of aggregates to colloidal P (CR) in the total 15 soils

	Size of aggregates (mm)	S1	S2	S3	S4	S5	S6	S7	S8	S9	S10	S11	S12	S13	S14	S15
Colloidal P	2–8	14.04a	1.25b	2.05d	11.35a	2.28d	3.00a	6.10a	11.01b	9.87c	1.48b	1.78c	1.00d	5.89c	10.24b	16.35a
	0.26–2	15.55a	1.55a	7.22a	11.33a	6.25a	2.2b	8.98a	17.11a	23.63ab	1.27bc	3.85b	2.87b	5.31c	12.70a	12.50b
	0.053–0.26	6.88b	1.78a	7.10a	9.07b	4.48c	2.14c	8.82b	11.21b	22.68b	3.45a	1.57c	2.11c	17.83a	13.8a	10.17c
CR _i	<0.053	1.67c	0.86c	5.27b	5.55c	5.60b	3.45a	3.58c	5.55c	12.3c	1.00c	7.60a	4.50a	7.69b	10.22ab	15.24a
	2–8	4.46c	2.17c	1.52d	4.10c	0.83c	4.43d	5.37b	4.78d	3.86d	3.18d	4.39b	2.58d	3.96c	6.25d	11.33a
	0.26–2	10.75b	11.72a	7.03c	11.02b	5.05b	5.88c	10.29a	12.30a	5.39c	4.51c	6.18a	5.64b	4.51b	7.61c	5.51c
	0.053–0.26	9.47b	12.86a	10.27b	10.17b	14.37a	7.98b	9.66a	7.41c	10.38a	5.82b	2.04c	4.17c	9.34a	9.81b	2.69d
	<0.053	26.14a	11.28a	15.92a	20.79a	15.06a	19.87a	4.43b	9.11b	9.21a	8.04a	4.07b	8.80a	8.32a	10.37a	7.11b

Letters in different-sized aggregates indicated significant difference at *P* < 0.05 level



Colloidal P content in aggregates

In this study, although no significant difference was observed in the P_{coll} fractions between different aggregate sizes in all soils, we observed that TDP, TSP, and P_{coll} contents in soil aggregates were significantly related to soil pH. The TDP and P_{coll} contents were high in macroaggregates of acidic soils, and low in microaggregates and silt + clay particles; however, contrasting results were observed in alkaline soil aggregates. This was not

consistent with our hypothesis which could be attributed to soil clays being mostly negatively charged, but the aggregation of other soil colloids strongly depend on their surface charge, being favored when approaching their point of zero charge [59]. Under acidic conditions, the protonation of Fe-, Al-oxides, and organic matter in colloids results in positive charges, leading to their association with soil particles. However, the dissociation of Fe- and Al-hydroxyl and humic functional groups ($R-COOH$, $R-CH_2-OH$, $R-OH$) under alkaline conditions results in a negative charge in the colloid [59], which promotes the release of fine particulate P and colloidal substances, thus increasing the TDP and P_{coll} contents in small-sized aggregates and particles. On the other hand, the lower pH enhanced the adsorption of organic matter on the fine particles and masked the inorganic mineralogy, resulting in fewer chances of P carried by Fe- and Al-oxides [60–62]. In addition, we observed that the P_{coll} content in soil aggregates positively correlated with the aggregate-associated Al and Fe content. This was attributed to the greater contents of Fe and Al in acidic soil than in alkaline soil, and that the presence of Al and Fe oxides may have enhanced the adsorption of P and stabilization of soil aggregates [15, 31, 63]. Al and Fe oxides have been recognized as important carriers of P_{coll} [64–67].

Loss potential of colloidal P in aggregates

We observed that the CR value of (silt + clay)-sized particles was larger than that of aggregates of other sizes, while the CR of large macroaggregates was the lowest in most soils, indicating that the (silt + clay)-sized particles contribute more to the P_{coll} loss potential, while macroaggregates immobilized soil P_{coll} . Colloidal P is highly bound to Fe and Al on the surface of macroaggregates [15, 68], enabling the formation of a stable composite structure that can resist the shear force of pore flow [64, 65]. Similarly, soil macroaggregates can increase the adsorption of P_{coll} on the surface and reduce its mobility [26]. The ratio of P_{coll} to TDP reflects the release potential of P_{coll} in soil aggregates to soil solution. The high value indicates the high loss potential of P_{coll} . We observed a negative correlation between the TC and TN content and P_{coll}/TDP in aggregates, indicating that higher the TC and TN content, the less likely release of P_{coll} from the soil aggregates, which was further confirmed by the negative correlation between TC and P_{coll}/TDP in the regression model (Table 4). Studies had shown that C and N are important carriers of P_{coll} (most organics act as organic colloidal complexes) [28, 69, 70], and the organic matter could stabilize Al/Fe colloids [71]. Therefore, increasing the carbon content in soil aggregates could

Table 4 Results from correlation analyses and stepwise linear regressions of colloidal P and colloidal P/TDP in different-sized aggregates with soil aggregate-associated mean weight diameter (MWD), geometric mean diameter (GMD), pH, total carbon (TC), total nitrogen (TN), C/P, C/N, Al, Fe, and Ca

Indexes	Aggregate sizes	TC	TN	TP	pH	Al	Fe	Ca	C/P	C/N	MWD	GMD
Colloidal P	Total	0.151	0.134	0.706**	0.223*	0.220*	0.251**	0.269**	−0.424**	0.241*	0.224*	−0.101
	2–8 mm	0.302	0.328	0.769**	0.095	0.374*	0.464*	0.492**	−0.517**	0.118	0.136	−0.247
	0.26–2 mm	0.089	0.129	0.796**	0.012	0.277	0.317	0.142	−0.644**	0.102	0.102	−0.264
	0.053–0.26 mm	0.149	0.128	0.662**	0.311	0.204	0.190	0.085	−0.461*	0.295	0.290	−0.124
	<0.053 mm	0.282	0.101	0.344	0.631**	−0.115	−0.085	0.588**	0.127	0.541**	0.528**	0.189
Colloidal P/TDP	Total	−0.522**	−0.471**	0.026	−0.301*	0.474**	0.365**	−0.373**	−0.449**	−0.298*	−0.072	−0.056
	2–8 mm	−0.509	−0.452	0.315	−0.387	0.764**	0.707**	−0.441	−0.807**	−0.435	−0.048	−0.030
	0.26–2 mm	−0.645**	−0.547*	0.147	−0.436	0.741**	0.513	−0.688**	−0.632*	−0.411	−0.090	−0.097
	0.053–0.26 mm	−0.485	−0.429	−0.008	−0.435	0.515*	0.458	−0.711**	−0.364	−0.234	−0.082	−0.025
	<0.053 mm	−0.386	−0.455	−0.322	0.107	0.247	0.104	0.261	−0.013	0.002	−0.074	−0.086
Stepwise linear regression	Colloidal P			Stepwise linear regression			Colloidal P/TDP			Stepwise linear regression		
	R^2	F	P				R^2	F	P			
	0.605	44.116	<0.001				0.539	16.058	<0.001			
	B	t	P				B	t	P			
(Constant)	−8.017	−2.979	0.004	(Constant)	0.478	2.98	0.004					
Al	0.087	3.235	0.018	TC	−0.028	−6.947	<0.001					
TP	10.598	3.88	<0.001	Fe	0.015	4.883	<0.001					
TN	−2.257	3.634	0.004	MWD	0.413	3.911	<0.001					
MWD	5.977	−2.651	<0.001	GMD	−0.363	−2.057	0.044					

Total total soil aggregate sizes

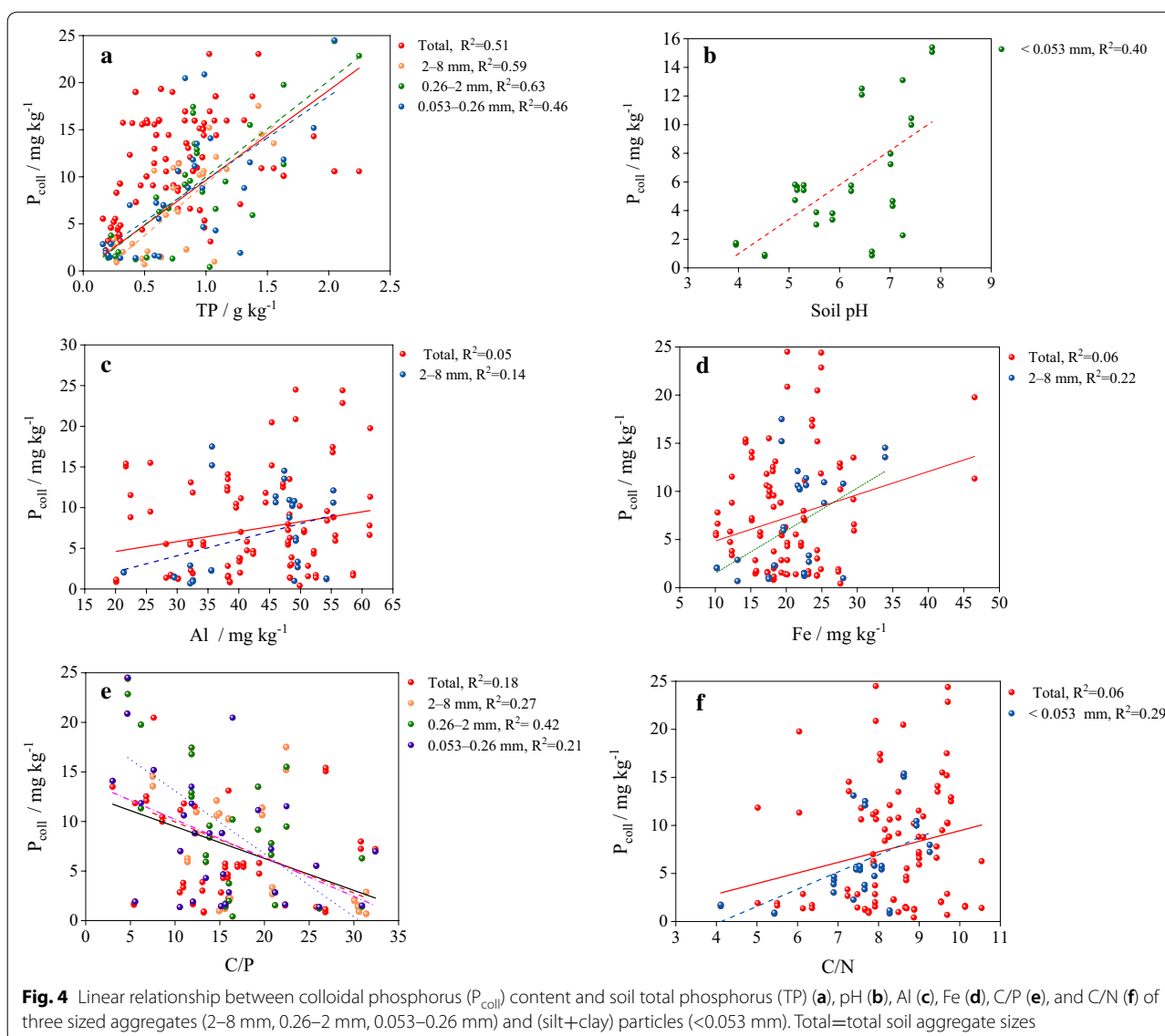
* $P < 0.05$, ** $P < 0.01$

be an important strategy to reduce the migration of P_{coll} in the soil. The ratio of P_{coll} to TDP for all macroaggregates in paddy soils was lower, which may be related to the long-term flooding of rice fields. Notably, the lower loss potential of P_{coll} in macroaggregates of paddy soils does not imply that it is less likely to be lost to water bodies. However, this could indicate that P_{coll} has been lost into water and discharged into the water body through the channels during rice seasons, particularly when under long-term flooding [72]. Moreover, flooding resulted in an anaerobic state in soil aggregates, and Fe bound to colloids and aggregates was reduced, resulting in excessive release and loss of P_{coll} [15]. We observed that aggregates of all sizes in dryland and rice–dryland rotation systems carried higher P_{coll} loss potential. Conversely, in paddy soils, the loss potential of P_{coll} in macro- and microaggregates was lower than 50% of TDP. However, P_{coll} in (silt + clay)-sized particles (<0.053 mm) in paddy soils accounted for a TDP proportion as high as 83%, significantly higher than that observed in orchard and rice–dryland rotation

systems. Therefore, we believe that P_{coll} in paddy soil is mainly carried by small silt and clay particles, which may indicate that the loss of P_{coll} is markedly severe in paddy soils.

Conclusions

This study discussed the relationship between P_{coll} and soil aggregates, providing a potential solution for soil P loss in agricultural systems. The soil P_{coll} content was affected by multiple factors including soil Al, Fe, and TP, and the distribution of P_{coll} in aggregates can be regulated by altering aggregate sizes and soil pH. As small macroaggregates contributed the most to the immobilization of P_{coll} , it is important to increase this fraction in the soil. To this end, soil organic matter must be improved owing to its crucial role in promoting soil aggregation and reducing the risk of P_{coll} loss potential. Paddy soils, due to their high P_{coll} /TDP ratio, are particularly at risk of high P_{coll} loss through smaller particles and worthy of further attention.



Supplementary information

Supplementary information accompanies this paper at <https://doi.org/10.1186/s12302-020-0299-5>.

Additional file 1: Table S1. The total phosphorus (TP, g kg⁻¹), dissolved P (TDP, mg kg⁻¹), and truly soluble P (TSP, mg kg⁻¹) of different-sized soil aggregates in the total 15 soils. **Table S2.** Correlation analysis of colloidal P in TP in soil aggregates and soil aggregate associated MWD, GMD, pH, TC, TN, C/N, C/P, Al, Fe, and Ca (n=45). MWD = mean weight diameter, MWD = mean weight diameter, TC = total C, TN = total N. **Figure S1.** Water-stable aggregate (WSA) and Dry soil aggregates (DSA) fractions of soils. **Figure S2.** Mean weight diameter (MWD) and geometric mean diameter (WMD) of different soil aggregates. Letters indicated significant difference among soils at P < 0.05 level.

Abbreviations

P: Phosphorus; P_{coll}: Colloidal phosphorus; TP: Total phosphorus; TC: Total carbon; TN: Total nitrogen; TDP: Total dissolved P; TSP: Truly soluble P; WSA:

Water-stable aggregate; MWD: Mean weight diameter; DSA: Dry soil aggregate; GMD: Geometric mean diameter; CR: Contribution rate.

Acknowledgements

We highly appreciate the reviewers and the handling editor for their helpful comments improving the quality and clarity of this work. We are grateful for grants from National Key Research and Development Program of China (2017YFD0800103); National Natural Science Foundation of China (41671300; 41522108); National Key Science and Technology Project: Water Pollution Control and Treatment (2018ZX07208009); Natural Science Foundation of Zhejiang Province (LR16B070001).

Authors' contributions

FYL is the first author of this article; XQL is the corresponding author and designed this study; FYL, MMH, YBJ, HL and JJW completed experiment and conducted data analysis. EK and RB provided specific guidance on this research and revised this MS. All authors helped to write the manuscript. All authors read and approved the final manuscript.

Funding

National Key Research and Development Program of China (2017YFD0800103); National Natural Science Foundation of China (41671300; 41522108); National Key Science and Technology Project: Water Pollution Control and Treatment (2018ZX07208009); Natural Science Foundation of Zhejiang Province (LR16B070001).

Availability of data and materials

The datasets used and/or analyzed during the current study are available from the corresponding author on reasonable request.

Ethics approval and consent to participate

Not applicable.

Consent for publication

Not applicable.

Competing interests

The authors declare that they have no competing interests.

Author details

¹ College of Environmental and Resources Sciences, Zhejiang University, Hangzhou 310058, China. ² College of Water Resources and Architectural Engineering, Tarim University, Xinjiang 843300, China. ³ Institute of Environment, Resource, Soil and Fertilizer, Zhejiang Academy of Agricultural Sciences, Hangzhou 310021, China. ⁴ Department of Life and Environmental Science, Hangzhou Normal University, Hangzhou 310036, China. ⁵ Institute of Bio- and Geosciences, Agrosphere (IBG-3), Forschungszentrum Jülich GmbH, 52425 Jülich, Germany. ⁶ Environment Centre Wales, Bangor University, Deiniol Road, Bangor, Gwynedd LL57 2UW, UK.

Received: 23 December 2019 Accepted: 24 January 2020

Published online: 10 February 2020

References

- Le C, Zha Y, Li Y, Sun D, Lu H, Yin B (2010) Eutrophication of lake waters in China: cost, causes, and control. *Environ Manag* 45:662–668. <https://doi.org/10.1007/s00267-010-9440-3>
- Yu T, Dai D, Han XJ, He CD, Fu G, Wu FC (2019) Characterization of phosphorus accumulation and release using diffusive gradients in thin films (DGT)-linking the watershed to Taihu Lake, China. *Sci Total Environ* 673:347–356. <https://doi.org/10.1016/j.scitotenv.2019.04.102>
- Schmidt KR, Beek T, Dai XH, Dong BZ, Dopp E, Eichinger F, Hammers-Wirtz M, Haußmann R, Holbach A, Hollert H, Illgen M, Jiang X, Koehler J, Koester S, Korth A, Kueppers S, Li AL, Lohmann M, Moldaenke C, Norra S, Qin BQ, Qin YW, Reese M, Riehle E, Santiago-Schuebel B, Schaefer C, Simon A, Song YH, Staaks C, Steinhardt J, Subklew G, Tao T, Wu TF, Yin DQ, Zhao FF, Zheng BH, Zhou MY, Zou H, Zuo J, Tiehm A (2016) Since 2015 the SinoGerman research project SIGN supports water quality improvement in the Taihu region, China. *Environ Sci Eur* 28:24. <https://doi.org/10.1186/s12302-016-0092-7>
- Li D, Wu N, Tang S, Su G, Li X, Zhang Y, Wang G, Zhang J, Liu H, Hecker MJ, Giesy JP, Yu HX (2018) Factors associated with blooms of cyanobacteria in a large shallow lake, China. *Environ Sci Eur* 30:27. <https://doi.org/10.1186/s12302-018-0152-2>
- Liang X, Jin Y, Zhao Y, Wang Z, Yin R, Tian G (2016) Release and migration of colloidal phosphorus from a typical agricultural field under long-term phosphorus fertilization in southeastern China. *J Soils Sediments* 16:842–853. <https://doi.org/10.1007/s11368-015-1290-4>
- Kretzschmar RBM, Grolimund D, Elimelech M (1999) Mobile subsurface colloids and their role in contaminant transport. *Adv Agron* 66:121–193. [https://doi.org/10.1016/S0065-2113\(08\)60427-7](https://doi.org/10.1016/S0065-2113(08)60427-7)
- Norgaard T, Moldrup P, Ferre TP, Katuwal S, Olsen P, de Jonge LW (2014) Field-scale variation in colloid dispersibility and transport: multiple linear regressions to soil physico-chemical and structural properties. *J Environ Qual* 43:1764–1778. <https://doi.org/10.2134/jeq2013.12.0510>
- Heathwaite L, Haygarth P, Matthews R, Preedy N, Butler P (2005) Evaluating colloidal phosphorus delivery to surface waters from diffuse agricultural sources. *J Environ Qual* 34:287–298. <https://doi.org/10.2134/OTTS71242>
- Hens M, Merckx R (2001) Functional characterization of colloidal phosphorus species in the soil solution of sandy soils. *Environ Sci Technol* 35:493–500. <https://doi.org/10.1021/es0013576>
- de Jonge LW, Kjærsgaard C, Moldrup P (2004) Colloids and colloid-facilitated transport of contaminants in soils. *Vadose Zone J* 3:321–325. <https://doi.org/10.2136/vzj2004.0321>
- Mayer T, Jarrell W (1995) Assessing colloidal forms of phosphorus and iron in the Tualatin River Basin. *J Environ Qual* 24:1117–1124. <https://doi.org/10.2134/jeq1995.00472425002400060010x>
- Shi P, Arter C, Liu X, Keller M, Schulin R (2017) Soil aggregate stability and size-selective sediment transport with surface runoff as affected by organic residue amendment. *Sci Total Environ* 607:95–102. <https://doi.org/10.1016/j.scitotenv.2017.07.008>
- Whalen JK, Chang C (2002) Macroaggregate characteristics in cultivated soils after 25 annual manure applications. *Soil Sci Soc Am J* 66:1637–1647. <https://doi.org/10.1007/s10705-007-9130-6>
- Wortmann C, Shapiro C (2008) The effects of manure application on soil aggregation. *Nutr Cycling Agroecosyst* 80:173–180. <https://doi.org/10.1007/s10705-007-9130-6>
- Henderson R, Kabengi N, Mantripragada N, Cabrera M, Hassan S, Thompson A (2012) Anoxia-induced release of colloid- and nanoparticle-bound phosphorus in grassland soils. *Environ Sci Technol* 46:11727–11734. <https://doi.org/10.1021/es302395r>
- Bradford SA, Yates SR, Bettahar M, Simunek J (2002) Physical factors affecting the transport and fate of colloids in saturated porous media. *Water Resour Res*. <https://doi.org/10.1029/2002WR001340>
- DeNovio NM, Saiers JE, Ryan JN (2004) Colloid movement in unsaturated porous media. *Vadose Zone J* 3:338–351. <https://doi.org/10.2136/vzj2004.0338>
- Lægdsmand M, de Jonge LW, Moldrup P (2005) Leaching of colloids and dissolved organic matter from columns packed with natural soil aggregates. *Soil Sci* 170:13–27. <https://doi.org/10.2136/vzj2011.0070>
- Lægdsmand M, Moldrup P, de Jonge LW (2007) Modelling of colloid leaching from unsaturated, aggregated soil. *Eur J Soil Sci* 58:692–703. <https://doi.org/10.1111/j.1365-2389.2006.00854.x>
- Vendelboe AL, Schjønning P, Moldrup P, Jin Y, Merbach I, de Jonge LW (2012) Colloid release from differently managed loess soil. *Soil Sci* 177:301–309. <https://doi.org/10.1097/ss.0b013e3182506dd3>
- Vogel C, Mueller CW, Hoschen C, Buegger F, Heister K, Schulz S, Schlöter M, Kogel-Knabner I (2014) Submicron structures provide preferential spots for carbon and nitrogen sequestration in soils. *Nat Commun* 5:2947. <https://doi.org/10.1038/ncomms3947>
- Lekfeldt JDS, Kjærsgaard C, Magid J (2017) Long-term effects of organic waste fertilizers on soil structure, tracer transport, and leaching of colloids. *J Environ Qual* 46:862–870. <https://doi.org/10.2134/jeq2016.11.0457>
- Munkholm LJ, Schjønning P, Debosz K, Jensen HE, Christensen BT (2002) Aggregate strength and mechanical behaviour of a sandy loam soil under long-term fertilization treatments. *Eur J Soil Sci* 53:129–137. <https://doi.org/10.1046/j.1365-2389.2002.00424.x>
- Ranatunga TD, Reddy SS, Taylor RW (2013) Phosphorus distribution in soil aggregate size fractions in a poultry litter applied soil and potential environmental impacts. *Geoderma* 192:446–452. <https://doi.org/10.1016/j.geoderma.2012.08.026>
- Hao X, Chang C, Li X (2004) Long-term and residual effects of cattle manure application on distribution of P in soil aggregates. *Soil Sci* 169:715–728. <https://doi.org/10.1002/jpln.200320355>
- Garland G, Bünemann E, Oberson A, Frossard E, Snapp S, Chikowo R, Six J (2018) Phosphorus cycling within soil aggregate fractions of a highly weathered tropical soil: a conceptual model. *Soil Biol Biochem* 116:91–98. <https://doi.org/10.1016/j.soilbio.2017.10.007>
- Udom BE, Ogunwale JO (2015) Soil organic carbon, nitrogen, and phosphorus distribution in stable aggregates of an Ultisol under contrasting land use and management history. *J Plant Nutr Soil Sci* 178:460–467. <https://doi.org/10.1002/jpln.201400535>
- Jiang X, Bol R, Willbold S, Vereecken H, Klumpp E (2015) Speciation and distribution of P associated with Fe and Al oxides in aggregate-sized fraction of an arable soil. *Biogeosciences* 12:6443–6452. <https://doi.org/10.5194/bg-12-6443-2015>

29. Cui H, Ou Y, Wang L, Wu H, Yan B, Li Y (2019) Distribution and release of phosphorus fractions associated with soil aggregate structure in restored wetlands. *Chemosphere* 223:319–329. <https://doi.org/10.1016/j.chemosphere.2019.02.046>
30. Zhang M, He Z, Calvert D, Stoffella P, Yang X, Li Y (2003) Phosphorus and heavy metal attachment and release in sandy soil aggregate fractions. *Soil Sci Soc Am J* 67:1158–1167. <https://doi.org/10.2136/sssaj2003.1158>
31. Wang JG, Yang W, Yu B, Li ZX, Cai CF, Ma RM (2016) Estimating the influence of related soil properties on macro-and micro-aggregate stability in ultisols of south-central China. *Catena* 137:545–553. <https://doi.org/10.1016/j.catena.2015.11.001>
32. Rubæk GH, Guggenberger G, Zech W, Christensen BT (1999) Organic phosphorus in soil size separates characterized by phosphorus-31 nuclear magnetic resonance and resin extraction. *Soil Sci Soc Am J* 63:1123–1132. <https://doi.org/10.2136/sssaj1999.6351123x>
33. Wang S, He X, Ye S (2020) Soil aggregation and aggregate-associated carbon, nitrogen, and phosphorus under different aged tea (*Camellia sinensis* L.) plantations in hilly region of southern Guangxi, China. *Sci Hortic* 262:109007. <https://doi.org/10.1016/j.scienta.2019.109007>
34. Wu W, Zheng Z, Li T, He S, Zhang X, Wang Y, Liu T (2018) Distribution of inorganic phosphorus fractions in water-stable aggregates of soil from tea plantations converted from farmland in the hilly region of western Sichuan, China. *J Soil Sediment* 18:906–916. <https://doi.org/10.1007/s11368-017-1834-x>
35. Shekhabadi M, Mahmoudzadeh H, Mahboubi A, Gharabaghi B, Ahrens B (2014) Land use effects on phosphorus sequestration in soil aggregates in western Iran. *Environ Monit Assess* 186:6493–6503. <https://doi.org/10.1007/s10661-014-3869-4>
36. Huang R, Lan M, Liu J, Gao M (2017) Soil aggregate and organic carbon distribution at dry land soil and paddy soil: the role of different straws returning. *Environ Sci Pollut Res* 24:27942–27952. <https://doi.org/10.1007/s11356-017-0372-9>
37. Lu M, Yang M, Yang Y, Wang D, Sheng L (2019) Soil carbon and nutrient sequestration linking to soil aggregate in a temperate fen in North-east China. *Ecol Indic* 98:869–878. <https://doi.org/10.1016/j.ecoli.2018.11.054>
38. Li S, Zhang S, Pu Y, Li T, Xu X, Jia Y, Deng Q, Gong G (2016) Dynamics of soil labile organic carbon fractions and C-cycle enzyme activities under straw mulch in Chengdu Plain. *Soil Tillage Res* 155:289–297. <https://doi.org/10.1016/j.still.2015.07.019>
39. Wang X, Qi JY, Zhang XZ, Li SS, Virk AL, Zhao X, Xiao XP, Zhang HL (2019) Effects of tillage and residue management on soil aggregates and associated carbon storage in a double paddy cropping system. *Soil Tillage Res* 194:104339. <https://doi.org/10.1016/j.still.2019.104339>
40. Elliott ET (1986) Aggregate structure and carbon, nitrogen, and phosphorus in native and cultivated soils 1. *Soil Sci Soc Am J* 50:627–633. <https://doi.org/10.2136/sssaj1986.03615995005000030017x>
41. Totsche KU, Amelung W, Gerzabek MH, Guggenberger G, Klump E, Knief C, Lehnendorff E, Mikutta R, Peth S, Prechtel A (2018) Microaggregates in soils. *J Plant Nutr Soil Sci* 181:104–136. <https://doi.org/10.1002/jpln.201600451>
42. Sumner ME, Miller WP (1996) Cation exchange capacity and exchange coefficients. *Methods Soil Anal Part 3 Chem Methods* 5:1201–1229. <https://doi.org/10.1097/00010694-197006000-00009>
43. Walker T, Adams A (1958) Studies on soil organic matter: I. Influence of phosphorus content of parent materials on accumulations of carbon, nitrogen, sulfur, and organic phosphorus in grassland soils. *Soil Sci* 85:307–318. <https://doi.org/10.1097/00010694-195901000-00001>
44. Ilg K, Siemens J, Kaupenjohann M (2005) Colloidal and dissolved phosphorus in sandy soils as affected by phosphorus saturation. *J Environ Qual* 34:926–935
45. Beauchemin S, Simard R, Cluis D (1998) Forms and concentration of phosphorus in drainage water of twenty-seven tile-drained soils. *J Environ Qual* 27:721–728. <https://doi.org/10.2134/jeq1998.00472425002700030033x>
46. Beauchemin S, Simard R, Bolinder M, Nolin M, Cluis D (2003) Prediction of phosphorus concentration in tile-drainage water from the Montreal Lowlands soils. *Can J Soil Sci* 83:73–87. <https://doi.org/10.4141/S02-029>
47. Álvaro-Fuentes J, Cantero-Martínez C, López M, Paustian K, Denef K, Stewart C, Arrúe J (2009) Soil aggregation and soil organic carbon stabilization: effects of management in semiarid Mediterranean agroecosystems. *Soil Sci Soc Am J* 73:1519–1529. <https://doi.org/10.2136/sssaj2008.0333>
48. Van Bavel C (1950) Mean weight-diameter of soil aggregates as a statistical index of aggregation 1. *Soil Sci Soc Am J* 14:20–23. <https://doi.org/10.2136/sssaj1950.036159950014000C0005x>
49. Wang W, Chen WC, Wang KR, Xie XL, Yin CM, Chen AL (2011) Effects of long-term fertilization on the distribution of carbon, nitrogen and phosphorus in water-stable aggregates in paddy soil. *Agric Sci China* 10:1932–1940. [https://doi.org/10.1016/S1671-2927\(11\)60194-6](https://doi.org/10.1016/S1671-2927(11)60194-6)
50. Adesodun J, Adeyemi E, Oyegoke C (2007) Distribution of nutrient elements within water-stable aggregates of two tropical agro-ecological soils under different land uses. *Soil Tillage Res* 92:190–197. <https://doi.org/10.1016/j.still.2006.03.003>
51. Wang S, Li T, Zheng Z (2018) Tea plantation age effects on soil aggregate-associated carbon and nitrogen in the hilly region of western Sichuan, China. *Soil Tillage Res* 180:91–98. <https://doi.org/10.1016/j.still.2018.02.016>
52. Edwards A, Bremner J (1967) Microaggregates in soils 1. *J Soil Sci* 18:64–73. <https://doi.org/10.1111/j.1365-2389.1967.tb01488.x>
53. Bronick CJ, Lal R (2005) Soil structure and management: a review. *Geoderma* 124:3–22. <https://doi.org/10.1016/j.geoderma.2004.03.005>
54. Awad YM, Lee SS, Kim K-H, Ok YS, Kuzyakov Y (2018) Carbon and nitrogen mineralization and enzyme activities in soil aggregate-size classes: effects of biochar, oyster shells, and polymers. *Chemosphere* 198:40–48. <https://doi.org/10.1016/j.chemosphere.2018.01.034>
55. Giaveno C, Celi L, Richardson AE, Simpson RJ, Barberis E (2010) Interaction of phytases with minerals and availability of substrate affect the hydrolysis of inositol phosphates. *Soil Biol Biochem* 42:491–498. <https://doi.org/10.1016/j.soilbio.2009.12.002>
56. George TS, Simpson RJ, Gregory PJ, Richardson AE (2007) Differential interaction of *Aspergillus niger* and *Peniophora lycii* phytases with soil particles affects the hydrolysis of inositol phosphates. *Soil Biol Biochem* 39:793–803. <https://doi.org/10.1016/j.soilbio.2006.09.029>
57. Yang Y, Liu S, Wang H, Chen L, Lu L, Cai D (2019) Reduction in throughfall reduces soil aggregate stability in two subtropical plantations. *Eur J Soil Sci* 70:301–310. <https://doi.org/10.1111/ejss.12734>
58. He Y, Gu F, Xu C, Chen J (2019) Influence of iron/aluminum oxides and aggregates on plant available water with different amendments in red soils. *J Soil Water Conserv* 74:145–159. <https://doi.org/10.2489/jswc.74.2.145>
59. Douch J, Hamdani M, Fessi H, Elaissari A (2009) Acid–base behavior of a colloidal clays fraction extracted from natural quartz sand: effect of permanent surface charge. *Colloids Surf A* 338:51–60. <https://doi.org/10.1016/j.colsurfa.2008.12.034>
60. Liang X, Liu J, Chen Y, Li H, Ye Y, Nie Z, Su M, Xu Z (2010) Effect of pH on the release of soil colloidal phosphorus. *J Soil Sediment* 10:1548–1556. <https://doi.org/10.1007/s11368-010-0275-6>
61. Kjaergaard C, Hansen HCB, Koch CB, Villholth K (2004) Properties of water-dispersible colloids from macropores and bulk horizons of an Agradalf. *Soil Sci Soc Am J* 68:1844–1852. <https://doi.org/10.2136/sssaj2004.1844>
62. Klitzke S, Lang F, Kaupenjohann M (2008) Increasing pH releases colloidal lead in a highly contaminated forest soil. *Eur J Soil Sci* 59:265–273. <https://doi.org/10.1111/j.1365-2389.2007.00997.x>
63. Barral M, Arias M, Guerif J (1998) Effects of iron and organic matter on the porosity and structural stability of soil aggregates. *Soil Tillage Res* 46:261–272. [https://doi.org/10.1016/S0167-1987\(98\)00092-0](https://doi.org/10.1016/S0167-1987(98)00092-0)
64. Cui Y, Xiao R, Xie Y, Zhang M (2018) Phosphorus fraction and phosphate sorption-release characteristics of the wetland sediments in the Yellow River Delta. *Phys Chem Earth Parts A/B/C*. 103:19–27. <https://doi.org/10.1016/j.pce.2017.06.005>
65. Gottselig N, Amelung W, Kirchner JW, Bol R, Eugster W, Granger SJ, Hernández-Crespo C, Herrmann F, Keizer JJ, Korkiakoski M (2017) Elemental composition of natural nanoparticles and fine colloids in European forest stream waters and their role as phosphorus carriers. *Global Biogeochem Cycles* 31:1592–1607. <https://doi.org/10.1002/2017GB005657>
66. Liu J, Yang JJ, Liang XQ, Zhao Y, Cade-Menun BJ, Hu YF (2014) Molecular speciation of phosphorus present in readily dispersible colloids from agricultural soils. *Soil Sci Soc Am J* 78:47–53. <https://doi.org/10.2136/sssaj2013.05.0159>

67. Petter FA, Madari BE, Silva MASd, Carneiro MAC, Carvalho MTdM, Júnior BHM, Pacheco LP (2012) Soil fertility and upland rice yield after biochar application in the Cerrado. *Pesqui Agropecu Bras* 47:699–706. <https://doi.org/10.1590/S0100-204X2012000500010>
68. van der Grift B, Osté L, Schot P, Kratz A, van Popta E, Wassen M, Griffioen J (2018) Forms of phosphorus in suspended particulate matter in agriculture-dominated lowland catchments: Iron as phosphorus carrier. *Sci Total Environ* 631:115–129. <https://doi.org/10.1016/j.scitotenv.2018.02.266>
69. Gottselig N, Nischwitz V, Meyn T, Amelung W, Bol R, Halle C, Vereecken H, Siemens J, Klumpp E (2017) Phosphorus binding to nanoparticles and colloids in forest stream waters. *Vadose Zone J*. <https://doi.org/10.2136/vzj2016.07.0064>
70. Missong A, Bol R, Nischwitz V, Krüger J, Lang F, Siemens J, Klumpp E (2018) Phosphorus in water dispersible-colloids of forest soil profiles. *Plant Soil* 427:71–86. <https://doi.org/10.1007/s11104-017-3430-7>
71. Pokrovsky OS, Dupré B, Schott J (2005) Fe–Al-organic colloids control of trace elements in peat soil solutions: results of ultrafiltration and dialysis. *Aquat Geochem* 11:241–278. <https://doi.org/10.1007/s10498-004-4765-2>
72. Leon A, Kohyama K (2017) Estimating nitrogen and phosphorus losses from lowland paddy rice fields during cropping seasons and its application for life cycle assessment. *J Cleaner Prod* 164:963–979. <https://doi.org/10.1016/j.jclepro.2017.06.116>

Publisher's Note

Springer Nature remains neutral with regard to jurisdictional claims in published maps and institutional affiliations.

Submit your manuscript to a SpringerOpen[®] journal and benefit from:

- Convenient online submission
- Rigorous peer review
- Open access: articles freely available online
- High visibility within the field
- Retaining the copyright to your article

Submit your next manuscript at ► [springeropen.com](https://www.springeropen.com)